

PAPER • OPEN ACCESS

Research on Control Strategy of Islanded Hybrid Microgrid Based on Hybrid Energy Storage

To cite this article: Shudong Wang *et al* 2018 *IOP Conf. Ser.: Earth Environ. Sci.* **199** 052049

View the [article online](#) for updates and enhancements.

You may also like

- [Research on capacity optimization configuration of AC/DC hybrid microgrid interconnect converter](#)
Zicong Yu, Yuan Tian, Zhi Wang et al.
- [Optimal Energy Sharing in Hybrid Microgrid System Using Battery Energy Storage](#)
Arun Kumar Rawat, Subhash Chandra and Vinay Kumar Deolia
- [Multi-time Optimal Dispatch of AC-DC Hybrid Microgrid with Spatiotemporal Discrepancy](#)
Hao Chen, Yi Lin and Chuangxin Guo



ECS
The
Electrochemical
Society
Advancing solid state &
electrochemical science & technology

DISCOVER
how sustainability
intersects with
electrochemistry & solid
state science research

Research on Control Strategy of Islanded Hybrid Microgrid Based on Hybrid Energy Storage

Shudong Wang¹, Jinliang Qiu¹, Liyang Zhu¹, Tin Ding¹ and AL-MADHEHAGI LUAI¹

¹College of Electrical and Information Engineering, Lanzhou University of Technology, Lanzhou, Gansu, 730050, China

*Corresponding author's e-mail: qiu_j_l@163.com

Abstract. In order to solve the power fluctuation and power balance problem in the AC / DC hybrid microgrid, a control strategy is proposed to dynamically adjust the output power of the bidirectional AC/DC converter connected to the AC and DC microgrid by detecting the DC voltage and the AC voltage frequency. The established method can be applied to different line impedances of AC power and load interconnections. In the hybrid energy storage, the droop control is used to automatically adjust the output power of the battery, and the supercapacitor quickly provides the high frequency component of the load power to reduce the impact caused by the load mutation on the battery and the bus voltage. Finally, a hybrid microgrid simulation model is built by using Matlab/Simulink. The simulation results show that the distributed control strategy can control the stable operation and voltage stability of the hybrid microgrid.

1. Introduction

In recent years, more and more renewable energy sources have been greatly utilized by accessing the microgrid. Microgrid can be divided into AC microgrid, DC microgrid and AC/DC hybrid microgrid from the grid structure and power supply mode[1]. In practical systems, many distributed power supplies (DG) typically output electrical energy in the form of DC, and the DC microgrid can directly supply DC loads, reducing frequent AC-DC conversion and providing high-quality power for DC loads[2-3]. In actual operation, the DC microgrid and the AC microgrid can be interconnected by a bidirectional AC/DC converter, and the converter can be controlled to achieve stable operation of the hybrid microgrid, thereby effectively reducing input cost and power loss, which can make full use of new energy generation[4-6]. Since the traditional power system is in the form of AC power supply, most of the existing researches focus on the operational control of the AC microgrid.

In order to coordinate the stable operation and voltage stability of hybrid microgrid, a new two-layer coordinated control strategy is proposed in [7]. In this strategy, the first layer controls the DC bus voltage and the AC current. The second layer controls the bus voltage drop problem dynamically to reduce the voltage fluctuation. However, the hierarchical control method has a high degree of dependence on communication. Once the communication fails, the system cannot operate normally. Reference [8] determines the reference active power of the AC/DC bidirectional power converter based on the frequency of the AC-MG and the voltage of the DC-MG, and achieves power balance by appropriately exchanging the active power. In [9], the expected transmission power through the interconnected converter is determined based on the unitized frequency variation in the AC-MG and the unitized voltage variation in the DC-MG and using a specific droop coefficient. In the above documents, the AC-MG adopts the P-f droop characteristic, but this control method is effective



only when it is assumed that the interconnection impedance between the load and the power source is purely inductive.

Based on the above analysis, this paper proposes an improved droop control strategy. By detecting the DC bus voltage and the AC voltage frequency, the output power of the bidirectional AC/DC is dynamically adjusted, and the reliability is high without relying on communication. At the same time, the battery in the hybrid energy storage system uses the droop control to adjust its active output, and the supercapacitor quickly provides the detected high-frequency component of the load power, thereby reducing the impact of sudden load changes on the busbar and the battery. In addition, feedforward compensation control is added to the AC load inverter to reduce fluctuations in the amplitude of the AC voltage when the disturbance occurs, thereby improving the quality of the supply voltage.

2. System structure and modelling

The hybrid microgrid structure studied in this paper is shown in Fig 1. It mainly consists of two parts: AC microgrid, DC microgrid, and interconnected by bidirectional AC/DC converters. The specific modelling is shown in Figure 1.

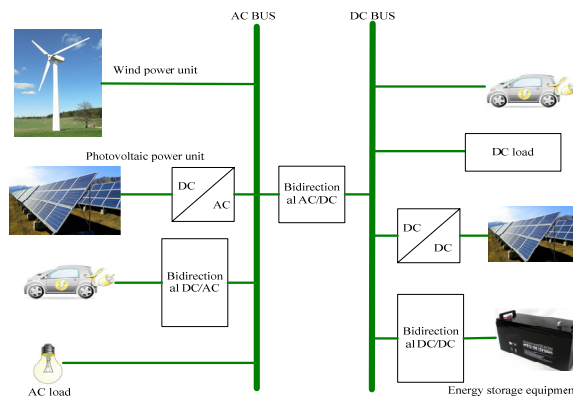


Figure. 1 Structure of islanded hybrid microgrid

2.1. Photovoltaic power generation system

In the AC subsystem, the photovoltaic power unit is connected to the AC bus through a DC/AC inverter to achieve MPPT and unit power factor control. In the DC subsystem, the photovoltaic power generation unit achieves maximum power tracking through the Boost converter. According to the equivalent circuit of the photovoltaic cell, the function equation of the photovoltaic cell can be obtained as

$$I = I_{ph} - I_d \left[e^{\frac{q(U+IR_s)}{AKT}} - 1 \right] - \frac{U + IR_s}{R_{sh}} \quad (1)$$

Where: U is the photovoltaic output voltage, I is the photovoltaic output current, I_{ph} is the photo-generated current of the photovoltaic panel, R_s and R_{sh} both represent the resistance, I_d the leakage current of the diode, T the temperature; q the amount of electron charge, A and k both are constant.

In photovoltaic power generation, the maximum power tracking control, MPPT control, is often used. In this paper, the Newton-Raphson iterative algorithm is used to solve the maximum power point current and voltage. The basic principle is to solve the equation (2) iteratively by applying the Newton-Raphson iterative method.

$$U_{k+1} = U_k - P'(U_k) / P''(U_k) \quad (2)$$

Where: U_{k+1} and U_k are the k th and $k+1$ th iteration values of U , respectively, $P'(U_k)$ and $P''(U_k)$ are the first and second derivatives of P to U under the k th iteration, respectively.

2.2. Wind power system

When the wind passes through the wind turbine, the wind energy is converted into kinetic energy and converted into mechanical power by the wind turbine rotor. The mechanical power absorbed by the wind turbine is

$$P = \frac{1}{2} \rho S v^3 C_p \quad (3)$$

Where: C_p is the wind energy utilization coefficient; v is the wind speed; S is the receiving area; ρ is the air density.

2.3. Energy storage system

As a storage device in distributed generation, the battery model commonly used is the Sheffield model, the Thevenin model and the general model. The battery model used in this paper is a general model, and the output voltage of the energy storage battery is

$$V_b = V_o + R_b i_b - K \frac{Q}{Q + \int i_b dt} + C \exp(B \int i_b dt) \quad (4)$$

$$SOC = 100 \left(1 + \frac{\int i_b dt}{Q} \right) \quad (5)$$

Where: R_b is the resistance of the battery; V_b and V_o are the battery output voltage and open circuit voltage; i_b is the charging current; K is the battery polarization voltage; Q is the battery capacity; K , B and C are constant.

3. Hybrid energy storage system control strategy

The battery plays an important role in buffering new power generation power fluctuations and control voltage stability. Since photovoltaic power generation and wind power generation have unstable power generation, battery storage energy is configured on the DC side, and battery charging is controlled by a bidirectional DC/DC converter. Discharge to suppress the wind/photovoltaic power generation and load power fluctuations, but because the battery responds slowly, by using the supercapacitor to quickly detect the abrupt part of the active power, it can effectively reduce the impact on the busbar and battery due to load fluctuations. At the same time, it can reduce the requirements on battery response speed and power density. In this paper, supercapacitors and accumulators are used to form a hybrid energy storage system to reduce voltage fluctuations while meeting dynamic response.

3.1. Analysis of main circuit of hybrid energy storage system

In the hybrid energy storage system shown in Figure 2, the supercapacitor is equivalently connected in series by capacitor C_{sc} and resistor R_{sc} , u_{sc} is its open circuit voltage, u_{bat} is the output voltage of the battery, and the half bridge converter 1 is composed of inductor L_1 , switch tube S_1 and S_2 and diodes VD_1 , VD_2 are constructed, the converter 2 is composed of an inductor L_2 , switching tubes S_3 and S_4 and diodes VD_3 , VD_4 respectively, i_{L1} , i_{L2} are the currents of the inductors L_1 , L_2 , respectively, u_{dc} and i_{dc} are the voltage and current of the load, Both i_{sco} and i_{bato} are output currents.

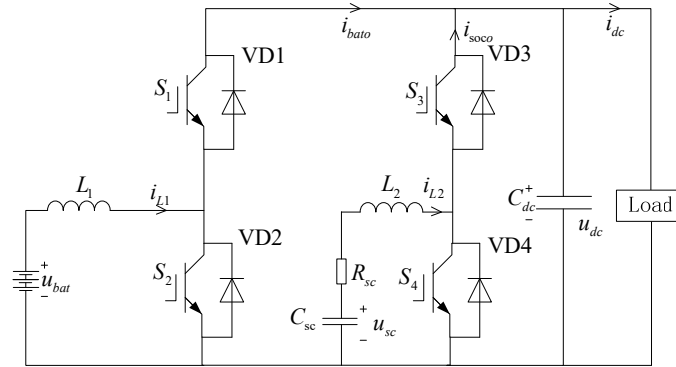


Figure. 2 Topology of hybrid energy storage system

The state space equation for a hybrid energy storage system is

$$\begin{cases} u_{L1} = L_1 \frac{di_{L1}}{dt} = \lambda(u_{bat} - \alpha u_{dc}) \\ C_{sc} \frac{du_{sc}}{dt} = -i_{L2} \end{cases} \quad (6)$$

$$\begin{cases} u_{L2} = L_2 \frac{di_{L2}}{dt} = \mu(u_{sc} - R_{sc}i_{L2} - \beta u_{dc}) \\ C_{dc} \frac{du_{dc}}{dt} = i_{bato} + i_{soco} - i_{dc} = \alpha i_{L1} + \beta i_{L2} - i_{dc} \end{cases} \quad (7)$$

Where: u_{L1} and u_{L2} are the voltages of inductors L_1 and L_2 respectively; λ , μ , α and β are taken according to the following principles.

- Converter 1 is in Boost mode, S_1 is off and S_2 is in the switch state. At this time, $\lambda=1$, $\alpha=1-d_2$, where d_2 indicates the duty cycle of S_2 in this mode.
- Converter 1 is in Buck mode, S_1 is in the switch state, S_2 is off, and $\lambda=-1$, $\alpha=d_1$, where d_1 is the duty cycle of S_1 in this mode.
- Converter 2 is in Boost mode, S_3 is off and S_4 is in the switch state. At this time, $\mu=1$, $\beta=1-d_4$, where d_4 indicates the duty cycle of S_4 in this mode.
- Converter 2 is in Buck mode, S_3 is in the switch state, S_4 is off, At this time, $\mu=-1$, $\beta=d_3$, where d_3 indicates the duty cycle of S_3 in this mode.

3.2. Hybrid energy storage system control strategy

The battery system uses droop control to automatically adjust the output power according to the load power demand to ensure bus voltage stability and buffer power fluctuations of distributed generation. The sagging characteristics of the battery sagging controller are

$$U_{dc} - I_{dc}Z_{dc} - U_{dc}^* = dP_{dc} \quad (8)$$

$$d = \frac{U_{dc}^{\min} - U_{dc}^{\max}}{P_{dc}^{\max}} \quad (9)$$

Where: Z_{dc} is the output impedance of the battery system; U_{dc}^* is the reference value of the DC bus voltage; U_{dc}^{\min} and U_{dc}^{\max} are the minimum and maximum output voltages of the converter 1; P_{dc}^{\max} is the maximum output power of the battery.

In the case of load power fluctuation, the single-pole high-pass filter is used to detect the high-frequency component of active power. The method is simple, reliable and easy to implement. Use P_{sref} to indicate the high frequency power component detected when the load fluctuates.

$$P_{scref} = U_{sc} \cdot I_{scref} \quad (10)$$

Further, the reference current of the converter 2 controller is

$$I_{scref} = \frac{P_{scref}}{U_{sc}} \quad (11)$$

The supercapacitor is the main device for smoothing the sudden high-frequency component of the load. It can withstand large charging currents and can quickly return energy. Combined with the detected high-frequency component of the active power of the load and equation (11), the controller current reference value of the supercapacitor can be obtained.

4. Hybrid microgrid control strategy

In the islanded mode, an improved droop control strategy is proposed for interconnected converters (ICs). The amount of active power transfer through the IC is determined by establishing a mathematical relationship. Different droop control can be used in consideration of the phase angle of the line impedance. In the case of overhead lines, the line impedance is almost a purely inductive load, $\theta = 90^\circ$, so P-f and Q-V droop control is used. The active power affects the system frequency, and the voltage amplitude is affected by the reactive power. However, in low-voltage cables where the phase angle is close to zero, the line is almost a resistive line and P-V and Q-f droop control should be used. To this end, this paper proposes $P-U_{ac}^P$ and $Q-U_{ac}^Q$ droop control strategies. U_{ac}^P and U_{ac}^Q are respectively defined as the AC microgrid unitized active and reactive power control index.

The active control index is determined for the AC-MG from the AC side. The AC-MG internal power output power formulas are (12) and (13):

$$P_{ac} = \left[\frac{E^2}{Z} - \frac{EV}{Z} \cos \delta \right] \cos \theta + \left[\frac{EV}{Z} \sin \delta \right] \sin \theta \quad (12)$$

$$Q_{ac} = \left[\frac{E^2}{Z} - \frac{EV}{Z} \cos \delta \right] \sin \theta + \left[\frac{EV}{Z} \sin \delta \right] \cos \theta \quad (13)$$

$E \angle \delta$ is the voltage amplitude and phase angle generated by the Voltage source inverter, $Z \angle \theta$ is the magnitude and phase angle of the line impedance, P_{ac} and Q_{ac} are the active and reactive power generated by the AC power source. The control index is calculated as equations (14) :

$$U_{ac}^P = \sin^2 \theta f_{ac}^* + \cos^2 \theta V_{ac}^* - (U_{\max} + U_{\min} - f_{ac}^* - V_{ac}^*) \sin 2\theta \cdot \frac{Q'_{\max,ac}}{P'_{\max,ac}} \quad (14)$$

f_{ac}^n and V_{ac}^n are the AC-MG unitized frequency and voltage, U_{\max} and U_{\min} are the allowable voltage maximum and minimum, and $P'_{\max,ac}$ and $Q'_{\max,ac}$ are the maximum active and reactive power generation capacity of the AC power source. It applies to any type of interface impedance in the AC-MG and can determine the amount of active power transfer through the IC. For purely inductive lines, U_{ac}^P are determined as frequency signal. In contrast, in the resistance line, U_{ac}^P are determined as voltage signal. From equation (13), it can be seen that U_{ac}^P depends on the phase angle of the line impedance. The ratio of the total reactive power to the total active power in the AC-MG, and the unitized voltage and frequency values. For the proposed strategy, measuring the voltage and frequency of the IC terminals is sufficient to control the AC and DC subnets. The measurement parameters are unitized on the AC side of the IC, and then brought into equation (14) to calculate the active power control index U_{ac}^P . Similarly, in the DC-MG, the corresponding active power control index U_{dc}^P is obtained by the measured voltage signal and unitization processing. The expected active power control index is calculated according to equation (15):

$$U_{des}^P = \frac{U_{ac}^P P_{max,ac}^t + U_{dc}^P P_{max,dc}^t}{P_{max,ac}^t + P_{max,dc}^t} \quad (15)$$

The amount of power transmitted through the IC can be determined according to the following formula:

$$\Delta P_{IC} = \frac{P_{max,ac}^t \cdot P_{max,dc}^t}{P_{max,ac}^t + P_{max,dc}^t} \frac{U_{ac}^P - U_{dc}^P}{\Delta U} \quad (16)$$

If $U_{ac}^P = U_{dc}^P = U_{des}^P$, the IC does not perform power transfer. In the case of $U_{ac}^P > U_{dc}^P$, power is transmitted from the AC-MG to the DC-MG. In contrast, in the case of $U_{ac}^P < U_{dc}^P$, power is transmitted from the DC-MG to the AC-MG.

5. Simulation results

In this paper, the micro-grid simulation model shown in Fig 1 is built. On the AC side, the rated active power of the AC side of the AC side is $P_{ac,e} = 10kW$ and the rated reactive power is $Q_{ac,e} = 5kVAR$. The no-load voltage on the AC side is $V_0^{ac} = 220V$, the allowable voltage variation range is $\Delta V_{ac} = 20V$, the AC side no-load frequency is $f_0 = 50HZ$, and the change frequency is allowed to $\Delta f = 1HZ$. On the DC side, the DC power supply has a rated active power of $P_{dc,e} = 10kW$. The no-load voltage on the DC side is $V_0^{dc} = 800V$, and the allowable voltage variation range is $\Delta V_{dc} = 80V$. The rated capacity of the battery is 4.5kWh. The bidirectional AC/DC power converter has a rated active power of $P_{ic,e} = 16kW$ and a rated reactive power of $Q_{ic,e} = 8kVAR$. In order to verify the performance of the proposed controller at different operating points, the load changes shown in Figure 3 are imposed on the system.

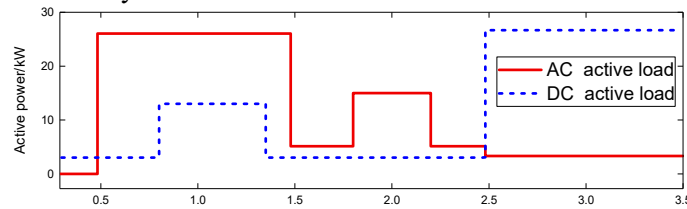


Figure.3 AC-MG and DC-MG active power requirements

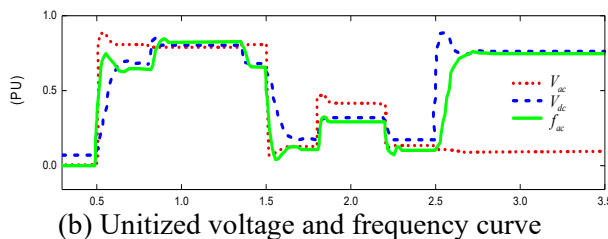
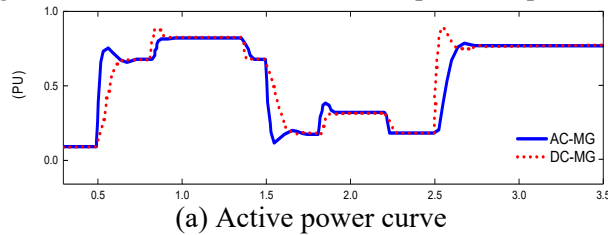


Figure.4 HMG simulation results of the proposed control strategy

Figure 4 shows the simulation results when using the proposed control strategy. Figure 4(a) shows the power generation curve for the micro power supply in AC-MG and DC-MG. It can be seen that any load change in the MG affects the power generation in the two MGs. According to the unitized active power of the AC and DC micro-power supplies in Figure 4a, the shared error of the active power can be observed. When the load variation fluctuates greatly, the power distribution will have a certain error, but within the allowable error range. The unitized voltage, frequency of the AC-MG and the unitized voltage in the DC-MG are shown in Figure 4b. The unitized active power parameters of the AC and DC micro-power supplies are equal, which can verify accurate active power sharing. Figure 5 shows the voltage of the common bus when using conventional control strategies and proposed control strategies. It can be seen that the proposed control strategy produces a lower voltage drop under heavy load conditions.

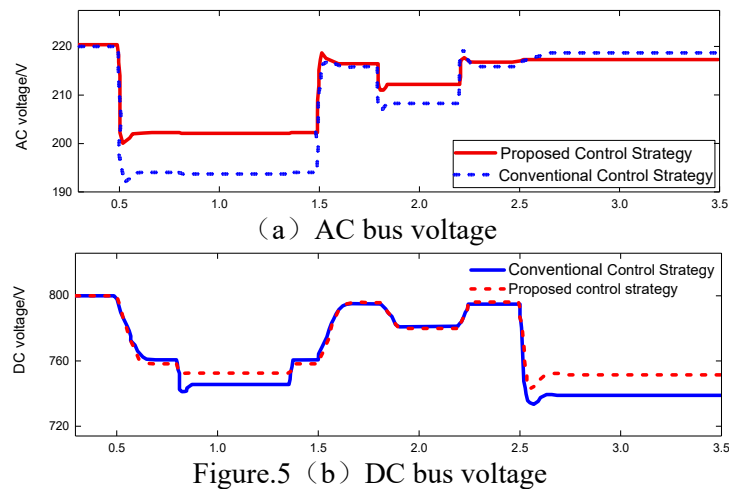


Figure.5 (b) DC bus voltage

6. Conclusion

In order to reduce power loss and coordinate the stable operation of hybrid microgrid, an improved droop control strategy based on hybrid energy storage is designed in this paper, which has low communication dependence and high reliability. The method has low communication dependence and high reliability. At the same time, the hybrid power supply of the battery and the supercapacitor is used to ensure the active power balance on the DC bus, and the voltage feedforward compensation amount is added to the droop controller of the load inverter to reduce the voltage fluctuation. In this paper, the effectiveness of the distributed control strategy is explored by Matlab/Simulink. The results show that the distributed control strategy can ensure the stable operation and voltage stability of the hybrid microgrid under different operating conditions.

References

- [1] Huang, Y.P., Ma, X.X. (2015) Research on Microgrid Technology. Transactions of China Electrotechnical Society, (s1): 320-328.
- [2] Zhu, S.S., Wang, F., Guo, H., et al. (2018) Overview of Droop Control in DC Microgrid. Proceedings of the CSEE, 38(1).
- [3] Han, M.X., Wang, H.J. (2015) DC Micro-grid—the Important Mode in the Field of Power Supply and Consumption. JOURNAL OF ELECTRICAL ENGINEERING, 10(5):1-9.
- [4] Jia, L.H., Zhu Y.Q., Du S.F., et al. (2016) Control Strategy of Interlinked Converter for AC DC Microgrid. Automation of Electric Power Systems, 40(24):98-104.
- [5] Ma, C.H., Pan Z.Y., Liu C.N., et al. (2015) Frequency regulation research of wind-PV-ES hybrid microgrid system based on adaptive droop control. Power System Protection and Control, (23):21-27.
- [6] Lan, Z., Tu, C.M., Xiao, F., et al. (2015) The Power Control of Power Electronic Transformer in Hybrid AC-DC Microgrid. Transactions of China Electrotechnical Society, 30(23):50-57.

- [7] LU, X.N., Sun, K., GURRERO J, et al. (2013) DC hierarchical control system for microgrid applications. *Transactions of China Electrotechnical Society*, 28(4): 35-42.
- [8] Loh, P.C., Li, D., Chai, Y.K., Blaabjerg, F. (2013) Autonomous operation of hybrid microgrid with AC and DC subgrids. *IEEE Trans Power Electron*, 28(5):2214-23.
- [9] Aryani, D.R., Song, H., (2016) Coordination Control Strategy for AC/DC Hybrid Microgrids in Stand-Alone Mode. *Energies*, 9(6):469.